Gyrotron-TWT Operating Characteristics

PATRICK E. FERGUSON, GERALD VALIER, AND ROBERT S. SYMONS, FELLOW, IEEE

Abstract—**The gyrotron traveling-wave tube (gyro-TWT) is a new type of millimeter amplifier which employs the electron cyclotron maser instability as a basis for the electron–electromagnetic wave interaction. A *C*-band gyro-TWT, employing the fundamental cyclotron resonance interaction with the circularly polarized TE_{11} dominant waveguide mode, has been constructed and tested. Initial power measurements yielded an output power of 50 kW at 60-kV beam voltage with 16.6-percent efficiency and 6-percent bandwidth. These measurements were recorded with a flat magnetic field. Subsequent experimental testing yielded, for a magnetic field increasing in magnitude towards the output portion of the tube, 128-kW and 65-kV beam voltage at 24-percent electronic efficiency. The maximum efficiency was 26 percent at 120.5-kW peak power, with an instantaneous bandwidth of 7.25 percent as measured in a high-beam power mode (65 kV, 7 A). In the low-beam power mode (40 kV, 4 A), the efficiency was 9.8 percent at 18.8-kW peak power at 9.3-percent instantaneous bandwidth. Additional experimental results of AM and PM modulation coefficients, spectral purity, phase linearity, and noise figure are presented.**

I. Introduction

THE GYROTRON traveling-wave tube (gyro-TWT) has received considerable theoretical and experimental attention as reported in the literature. The majority of the theoretical effort has been given to a gyro-TWT operating at 35 GHz in the TE_{01} circular electric mode at the fundamental electron cyclotron frequency [1]–[3].

Recently, at Varian Associates, Inc., a gyro-TWT operating in the TE_{11} dominant waveguide mode at approximately 5 GHz was reported [4]. Initial experimental results included measurements of stable gain as high as 24 dB small signal and 18 dB saturated. A saturated power output of 50 kW at a total beam efficiency of 16.6 percent was measured with a 3-dB saturated power output bandwidth of 6 percent at 60-kV beam voltage and 5-A beam current. Since the publication of the results for both the 35- and 5-GHz gyro-TWT, considerable interest has been shown toward radar and communication systems applications. It seemed appropriate then to characterize the 5-GHz gyro-TWT as to peak power output with various beam conditions, small signal and saturated gain, instantaneous bandwidth, maximum efficiency, amplitude modulation (AM) sensitivity and frequency modulation (FM) sensitivity to operating parameters, spectral purity, phase linearity, and noise figure.

A description of the gyro-TWT and a discussion of the associated magnetic-field configuration are given in Section II. In Section III the experimental results are presented. A summary is given in Section IV.

Manuscript received September 19, 1980; revised March 2, 1981. The development of gyro-TWT was supported under Contract with Rome Air Development Center, Griffiss Air Force Base, New York.

The authors are with Varian Associates, Inc., Palo Alto, CA 94303.

II. Device Description

Three gyro-TWT's were constructed and tested. All tubes used the fundamental cyclotron resonance interaction with the circularly polarized TE_{11} dominant waveguide mode. The tubes differed in the length of the single circuit section and in the amount of distributed loss.

The third gyro-TWT is shown in Fig. 1. The electron gun is of the magnetron-injection type, operating temperature-limited. This gun produced an annular electron beam with mean radius of 0.34 in in the interaction region. The area convergence is 4:1. The gun was designed to operate at 60-kV beam voltage and 5-A beam current with a perpendicular velocity ratio of 2:1 and a parallel velocity spread of 5-percent maximum. Early data [4] indicated that assuming a perpendicular velocity ratio of 1.5:1, reasonable agreement was obtained between the calculated and experimental small-signal gain. The calculated results were obtained with an assumed zero temperature beam, i.e., there was no spread in the parallel or perpendicular velocity components.

The input waveguide is rectangular with a low VSWR transition at the RF circuit junction. A second input guide orthogonal to the one shown was included in order to excite the two degenerate waves of the TE_{11} mode. This has not been accomplished to date. The output window is a 5-cm-diameter disk of alumina. The collector, being of slightly larger diameter, is insulated from the body of the tube. This change in diameter without impedance transformation unfortunately resulted in a mismatch which gave rise to some variation in the RF power spectrum.

The RF circuit of the gyro-TWT is a cylindrical waveguide of length 43 cm and diameter 3.7 cm. The first 67 percent of the circuit from the input end was coated with Kanthal. Kanthal is a lossy compound of iron, chromium, and aluminum. Insertion-loss measurements were performed to determine if the loss of Kanthal was magnetic-field dependent. The measurements indicated that the loss decreased linearly as a function of magnetic field up to 1900 G. The loss decreased by a factor of two. The loss remained constant above 1900 G. No hysteretic effects were found.

The arrangement of the six magnetic coils are as shown. Gun coil 1 is required for focusing the electron beam. This coil has very little effect on power output. Gun coil 2 aids

0018-9480/81/0800-0794$00.75 ©1981 IEEE

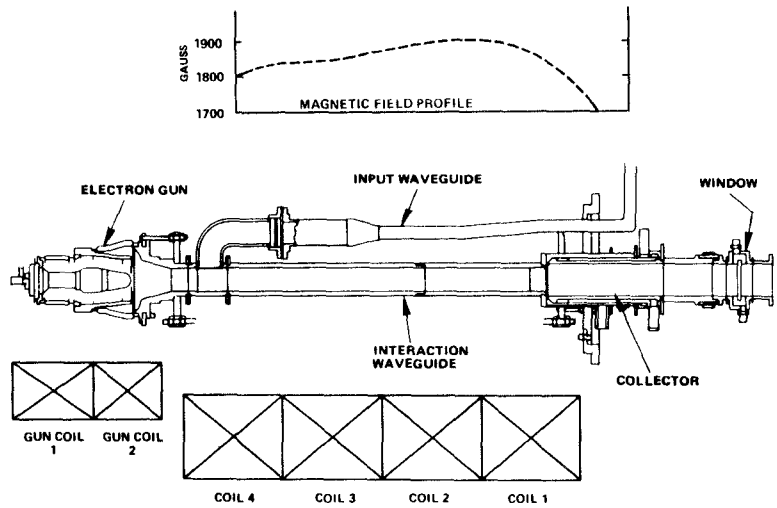

Fig. 1. Cross section of 5-GHz gyro-TWT with magnets.

in focusing and in the control of the magnitude of the perpendicular velocity in the beam. As the beam enters the RF interaction region, it undergoes adiabatic compression. Magnet 4 is very instrumental in obtaining high gain and power output. Magnet 1 is comparable in sensitivity to magnet 4 as to gain and power output. Magnets 2 and 3 are less influential than magnets 1 and 4. The main magnetic field profile as adjusted for maximum efficiency increases in magnitude by 4.4 percent from the input waveguide to the output end. The indicated positive slope in magnetic field is in qualitative agreement with theoretical predictions [5].

TABLE I
PREVIOUS EXPERIMENTAL RESULTS

Beam Voltage	60	kV
Beam Current	5	A
Frequency	5.2	GHz
Peak Output Power	50	kw
Small Signal Gain (Maximum)	24	dB
Saturated Gain	18	dB
Bandwidth	6	%
Efficiency	16.6	%

III. EXPERIMENTAL RESULTS

The first experimental measurements [4] on the gyro-TWT as discussed above are listed in Table I. Since these measurements were made, several changes have been made in the cathode pulsed test station and RF measuring system. One major change was in the replacement of the six nonregulated and nonisolated magnet power supplies with six current-regulated (1 part in 10^3) power supplies with ten-turn potentiometers. The ten-turn potentiometers allowed for very fine adjustment of the magnetic field. The currents through the six coils were measured using calibrated shunts with digital readout. Another improvement was the calibration *in situ* of the two capacitive dividers for measuring the cathode and mod-anode voltages. A calorimeter with integral thermopiles and digital readout was installed to measure RF output power. To substantiate the measured output power, the input and output waveguide systems were calibrated independently. Agreement within 0.2 dB was obtained across the operating band. The initial peak power measurements before the changes indicated that RF saturation was approached but not obtained over the operating band. A TWT driver with considerably more peak power was obtained. This additional input power was sufficient to obtain full saturation over a large proportion of the band.

RF compression curves of peak power out as a function of peak power in are shown in Figs. 2 and 3 for $f=5.18$ GHz and $f=5.20$ GHz, respectively. The small-signal gain of 26 dB and saturated gain of 20 dB as shown in Fig. 2 are of significance. The 26-percent electronic efficiency as shown in Fig. 3 represents the highest efficiency reported to date for a gyro-TWT. This efficiency was calculated from the relation of

$$\frac{\text{Peak Power Out} - \text{Peak Power In}}{\text{Peak Beam Power}}.$$

Peak power output versus frequency at two levels of beam power are displayed in Figs. 4 and 5. The purpose of measuring these data was to demonstrate the dual-mode capability of the gyro-TWT. For the high-beam power mode in Fig. 4, the peak power output is 120.5 kW and the instantaneous bandwidth as indicated is 7.25 percent. The RF power hole at 5.43 GHz is due to the impedance mismatch caused by the oversized collector. The elimination of this mismatch would give an instantaneous bandwidth of 8.8 percent for the high-power mode in comparison with the instantaneous bandwidth of 9.3 percent as shown in Fig. 5 for the lower-power mode. The measured results as shown represent the widest bandwidths reported for a gyro-TWT. It should be noted that, in spite of the fact that the magnetron gun was designed to operate at 60 kV at 5-A beam current, good performance has been obtained at 40 kV and 4 A to 65 kV and 8 A. The

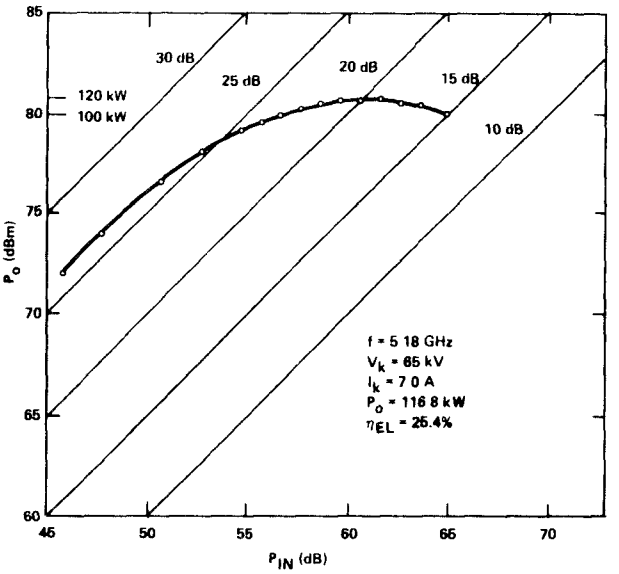

Fig. 2. Peak power output versus peak power input.

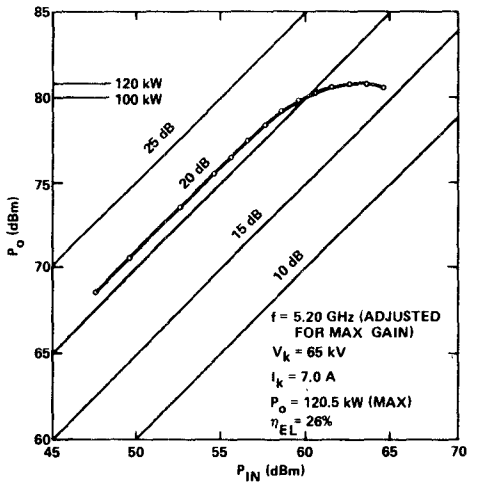

Fig. 3. Peak power output versus power input.

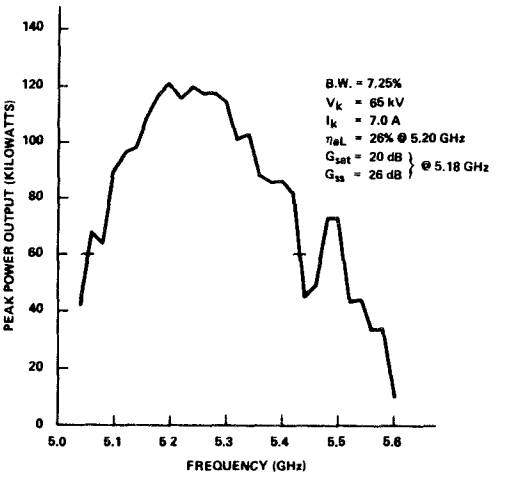

Fig. 4. Peak power output versus frequency (high-power mode).

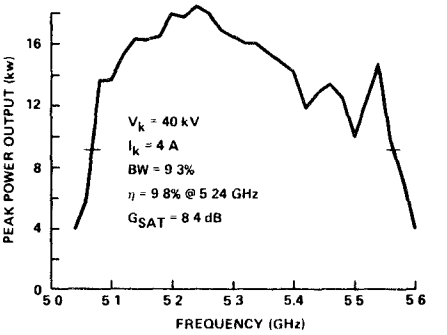

Fig. 5. Peak power output versus frequency (low-power mode).

TABLE II
FINAL EXPERIMENTAL POWER MEASUREMENTS

Beam Voltage	65	kV
Beam Current	8	A
Frequency	5.2	GHz
Peak Output Power	128	kw
Efficiency	24	%

TABLE III
AM PUSHING FACTORS

Parameter	Gyro-TWT (dB/%)	CC-TWT* (dB/%)
Cathode Voltage	0.045	0.5
Cathode Current	0.05	0.05
Mod. Anode Voltage	0.02	0.1
Main Magnetic Field	0.94	0.25

*10 kW, 5% BW, 60 dB gain

computer simulations made during the gun design indicated some sensitivity to the spread of perpendicular energies to the operating conditions. The wide range of operating parameters over which good performance has been obtained is somewhat surprising. It is possible that the high interaction impedance of the circularly polarized TE_{11} mode makes this gyro-TWT relatively insensitive to spread in the perpendicular and parallel velocities.

The final experimental power measurements are listed in Table II. At 65-kV beam voltage and 8-A beam current, a peak power of 128 kW at 24-percent efficiency was obtained. One of the major emphases in this study has been the measurement of saturated power, bandwidth, and efficiency. To data, due to the lack of a broad-band large-signal gain computer program, no calculations have been attempted to compare experiment with theory. The deviation and implementation of such a program is in progress.

A gyro-TWT designed to operate at 95.5-GHz center frequency is currently in development. The design of this amplifier has been scaled directly using the results listed in Table II.

AM sensitivities to operating parameters are listed in Table III. For comparison, data for a 10-kW coupled-cavity TWT with 5-percent bandwidth and 6-dB gain is also listed. As indicated, AM sensitivities are considerably lower

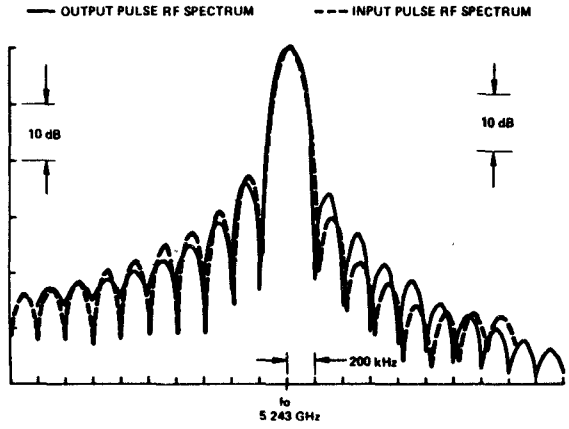

Fig. 6. Spectral measurements.

TABLE IV
PM PUSHING FACTORS

Parameter	Gyro-TWT	CC-TWT*
Cathode Voltage	4.2°/%	30°/%
Cathode Current	1.93°/%	0.001°/%
Mod. Anode Voltage	3.6°/%	7°/%
Main Magnetic Field	7.94°/%	2.5°/%
Drive Power	4°/dB Sat.	2.2°/dB
	7.25°/dB Lin.	

*10 kW, 5% BW, 60 dB gain

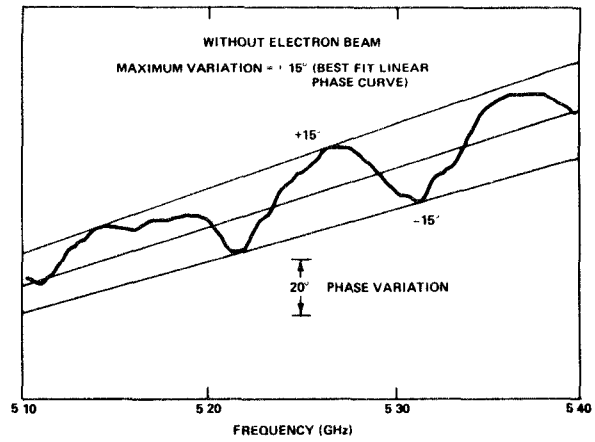

Fig. 7. Phase variation versus frequency.

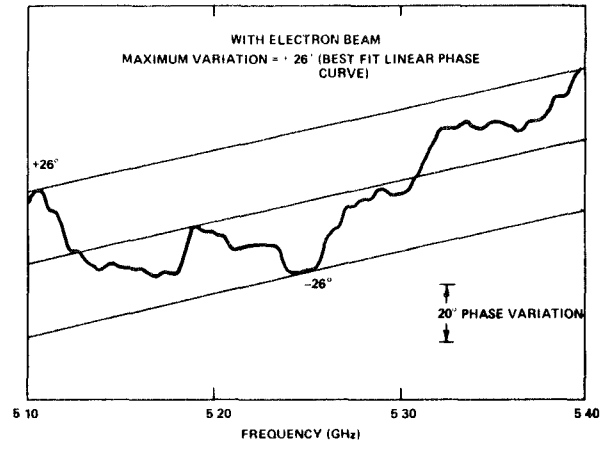

Fig. 8. Phase variation versus frequency.

for the gyro-TWT with regard to electron beam parameters. This is partially a result of the higher gain of the coupled-cavity TWT. The major contributor to AM is the variation in the main magnetic field. The magnetic field for this gyro-TWT was produced by a room-temperature electromagnet. For gyro-TWT's operating at a center frequency of 30 GHz or higher, the magnetic field would be produced by a superconducting solenoid. Under normal operating conditions, the superconducting solenoid would operate in the persistence mode, i.e., the external power supply would be essentially disconnected. Under these conditions, the main magnetic field would be almost constant and the AM would be negligible.

PM sensitivities to operating parameters are listed in Table IV. Data for the 10-kW coupled-cavity TWT is listed for comparison. PM due to variation in cathode voltage and modulating anode voltage is considerably less than for the coupled-cavity TWT. The variation in the main magnetic field is the major contributor to PM. For reasons cited above for AM sensitivity, it is considered that with an almost constant magnetic field from a super conducting solenoid, the PM would be negligible.

RF spectral purity tests were performed by examining both input and output RF pulse spectra by use of a spectrum analyzer. The pulse spectrum envelopes are shown in Fig. 6. Comparison of these spectra indicates no significant degradation. In fact, some improvement in symmetry is achieved, possibly due to the slope of the gyro-TWT voltage pulse compensating for the slower slope of the driver-TWT voltage pulse.

Phase versus frequency measurements were performed both with and without the electron beam. Without the beam, as shown in Fig. 7, the phase varies $\pm 15°$ from best fit linear phase line and shows some periodic variation. With the beam present, as shown in Fig. 8, the phase varies $\pm 26°$ from best fit linear phase line. In both cases, the phase variation should be reduced considerably by improved circuit matching.

The noise output of the gyro-TWT was measured in a somewhat unorthodox manner. Since it was anticipated that the noise figure of the amplifier would be in excess of 30 dB, the standard noise lamp technique of adding noise at the amplifier input would not be effective. Therefore, a technique was devised to measure the noise at the output of the gyro-TWT. A block diagram of the components is shown in Fig. 9. An argon noise source with nominal excess noise of 15 dB was used as a reference for calibration. The noise source output was gated by a p-i-n modulator to be present during the gyro-TWT interpulse period. A sample of the gyro-TWT output was coupled through a precision variable attenuator and RF coupler to add with the signal from the noise source. The combined signals

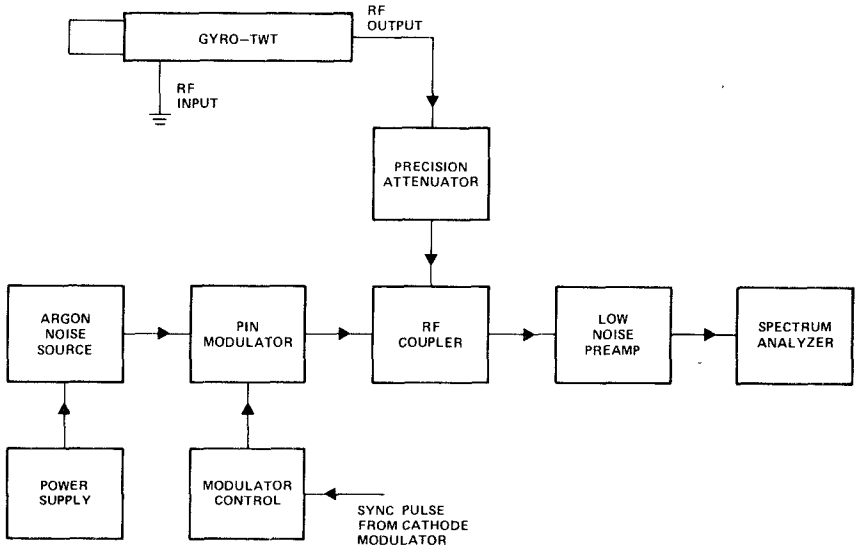

Fig. 9. Block diagram of noise-measuring apparatus.

TABLE V
NOISE FIGURE

Frequency	Noise Figure (Above Thermal)
5.05 GHz	56 dB
5.10	44
5.15	51.5
5.20	49
5.25	48
5.30	51
5.35	52
5.40	50
5.45	53
5.50	55

were amplified by a low-noise RF preamplifier and then displayed by the RF spectrum analyzer. With the spectrum analyzer set for zero sweep width, the comparative magnitudes of the noise source pulse and the gyro-TWT output noise pulse could be observed. By adjusting the calibrated attenuator to achieve equal amplitude of both pulses, the gyro-TWT output noise could be determined by adding the output coupling factor to the 15-dB excess noise from the argon lamp. This calculation yielded output noise with respect to thermal noise. Discrete frequencies in the operating band were obtained by manually tuning the RF spectrum analyzer in order to determine whether there existed a frequency dependency. The resulting data were then referred to the gyro-TWT RF input by subtracting the small-signal gain to obtain an effective input noise figure above thermal. These data are tabulated in Table V as a function of frequency. The noise figure rise at the band edges is probably a result of the output noise being rather constant with the small-signal gain being very low. In comparison, a coupled-cavity TWT operating at approximately the same beam and output power levels would exhibit a total noise figure 12–15 dB lower.

IV. Discussion

The characterization of a gyro-TWT has been presented in the interest of possible applications to radar and communication systems. The performance of the gyro-TWT has been shown to be comparable if not superior in many ways to a coupled-cavity TWT. A high-power–low-power capability, i.e., dual-mode operation, with almost the same bandwidth for each mode, has been demonstrated. Present-day coupled-cavity TWT's generally suffer considerable bandwidth compression when changing from the high-power mode to the low-power mode. It is considered that, for some high-power applications, a gyro-TWT, because of its simplicity, can be the proper economic choice.

Finally, consideration should be given to the scalability of the gyro-TWT to higher frequencies. The interaction circuit, being a simple cylindrical waveguide in which one or more modes can propagate, can be scaled directly. The problem of impedance matching and inserting lossy material for stability will become more complicated as the operating frequency increases and the physical dimensions decrease proportionally. The scaling of the magnetron-type injection electron gun to higher operating frequencies presents the most difficult problem. It has been shown herein that the gyro-TWT can be operated at different beam powers. However, if optimum efficiency and output power are to be obtained, it will be necessary to design the magnetron gun from fundamentals for each operating frequency since scaling laws cannot be used.

References

[1] K. R. Chu and A. T. Drobot, "Theory and single wave simulation of the gyrotron traveling wave amplifier operating at cyclotron harmonics," NRL Memo. Rep. 3788, Aug. 1978.

[2] K. R. Chu *et al.*, "Characteristics and optimum operating parameters of a gyrotron traveling wave amplifier," *IEEE Trans. Microwave*

Theory Tech., vol. MTT-27, pp. 178–187, 1979.
[3] L. R. Barnett *et al.*, "Gain, saturation and bandwidth measurements of the NRL gyrotron traveling wave amplifier," presented at the Int. Electron Devices Meet., Washington, DC, 1979.
[4] "High power millimeter wave amplifier," Phase II, Final Tech. Rep., Rome Air Development Center, Contract No. F30602-78-C-0011, Jan. 1980.
R. S. Symons *et al.*, "An experimental gyro-TWT," presented at the Int. Electron Devices Meet., Washington, DC, 1979.
[5] K. R. Chu, private communication.

Modeling and Characterization of Microstrip-to-Coaxial Transitions

MARIAN L. MAJEWSKI, MEMBER, IEEE, ROBERT W. ROSE, AND JAMES R. SCOTT, STUDENT MEMBER, IEEE

***Abstract*—A simple circuit model for the transition from a lossy microstrip to coaxial line has been developed on an experimental basis. The proposed model can be used to predict accurately the insertion loss and insertion phase over a wide frequency range.**

Since explicit formulas for the model element values are given, these elements, representing the parasitics of the transitions, can be taken into account very easily when the microstrip is used as a test fixture for measuring the parameters of solid-state devices. The practical use of the model has been examined for several $Z_0 = 50$-Ω lines on both Epsilam-10 and 99-percent alumina substrates with standard SMA coaxial connectors.

I. Introduction

A MODEL with empirically derived elements describing the parasitic reactances associated with conventional microstrip-to-coaxial line transitions is considered in this paper. A typical microstrip-to-coaxial transition unit is shown in Fig. 1.

A model, which is applicable to a wide range of microwave frequencies, has been developed from basic insertion phase relationships [1]. These relationships provide simple formulas from which the model components can be calculated. These formulas make the model easy to use for measurement and analysis purposes.

Alternate methods for performing parasitic component value calculations are available, for example Weissfloch's method [2]. However, these methods are, in general, more cumbersome than the simple computational methods proposed here, where the only computing aid required is a commonly available programmable calculator.

Manuscript received August 4, 1980; revised February 10, 1981. This work was supported by the Radio Research Board, Australia.

The authors are with the Department of Communication and Electronic Engineering, Royal Melbourne Institute of Technology, Melbourne, Vic., 3000, Australia.

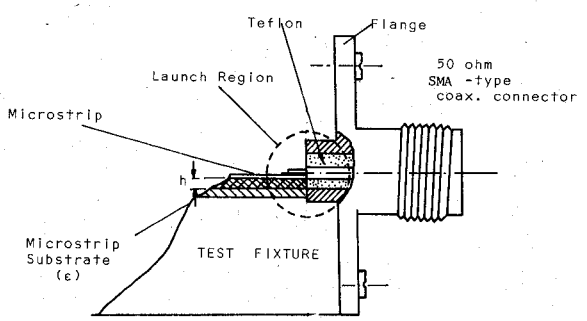

Fig. 1. Typical coaxial to microstrip transition.

For measurement purposes, it is usual for a solid-state device to be embedded in a microstrip network with the measurement reference planes being fixed at the coaxial terminations (see Fig. 1). However, to characterize accurately the device under test, it is necessary that the reference planes be transferred to the actual "ports" of the device. The values of the parasitic components introduced by the transition units must be known if they are to be accounted for in the measurement process.

The proposed model and the related measurement-calculation methods described here are very useful for this purpose, as they offer a quick and reliable characterization of the transition parasitics. They also take into account the microstrip attenuation constant α.

The practical use of the model has been examined for several $Z_0 = 50$-Ω lines on both Epsilam-10 and 99-percent alumina substrates with standard SMA-type coaxial connectors.[1]

[1]Sealectro SMA connector type 50-645-4546-31.

0018-9480/81/0800-0799$00.75 ©1981 IEEE